

Supporting information

Non-contact Electrochemical Imaging of Young's modulus of Single Living Cells

Rong Jin^{a, c†}, Yanyan Xu^{a, b†}, Kang Wang^a, Dechen Jiang^{a*}, Danjun Fang^{**b}

a. State Key Laboratory of Analytical for Life Science, School of Chemistry and Chemical Engineering, Nanjing University, Nanjing, 210023, China

b. School of Pharmacy, Nanjing Medical University, Nanjing, 211126, China

c. School of Chemistry and Chemical Engineering, Southeast University, Nanjing, 211189, China.

* Corresponding author. State Key Laboratory of Analytical for Life Science, School of Chemistry and Chemical Engineering, Nanjing University, Nanjing, 210023, China

** Corresponding author. School of Pharmacy, Nanjing Medical University, Nanjing, 211126, China

E-mail addresses: dechenjiang@nju.edu.cn (D. Jiang), djf@njmu.edu.cn (D. Fang)

† Rong Jin and Yanyan Xu contributed equally to this work.

List of content

Experimental section.	S3
Mathematical relation between ion current and sample modulus.	S7
COLSOL simulation using FEM model.	S10
Fig. S1. Schematic diagram of rotational axis symmetry of the FEM model.	S10
Table S1. The primary geometric parameters of the pipette's FEM.	S11
Table S2. Boundary conditions for the FEM model.	S11
Fig. S2. Simulation results of the hydrodynamic resistance.	S13
Fig. S3. The decay trend of hydrodynamic resistance and sample deformation.	S14
Fig. S4. Schematic diagram of the force transmission process during approaching.	S14
Fig. S5. Diagram of the morphology and modulus imaging destination.	S15

Fig. S6. SEM images of the nanocapillary.

S15

Fig. S7. Theoretical relationship and measured results of PDMS samples. S16

Fig. S8. The relationship between I_{\min} , η and ν . S16

Fig. S9. Approaching curves of different sites of the cell surface. S17

Fig. S10. Continuous morphology and modulus images of the same cell. S17

Fig. S11. Non-contact measurement characteristics verification. S18

Fig. S12. Statistical results of cell modulus before and after fixation. S18

Fig. S13. SICM modulus imaging results of a single SKOV3 cell. S19

Fig. S14. SICM modulus imaging results of the tiny area on SKOV3 cells. S19

Fig. S15. SICM morphology and modulus image of the PDMS standard array. S20

Fig. S16. Optical images of SKOV3 cells during the wound healing assay. S20

Fig. S17. Bright field image of the selected cell after fixation. S21

Experimental section

1.1. SICM setup

A home-built SICM was adopted in this work, including a scanning head on an optical microscope (Nikon Ti, Japan). Inside the scanning head, the movement in Z direction was separated from XY directions to decrease the location error. For X and Y directions, a piezo (P-621, PI Co., Germany) driven by a servo controller (E-509, PI Co., Germany) and a motor controller (C-863.11, PI Co., Germany) was installed on a stepping motor (M-111.1, PI Co., Germany). The sample stage was installed on XY-direction piezo. For Z direction, a piezo (P-753, PI Co., Germany) driven by a servo controller (E-509) was installed on a stepping motor (M-111.1) that was driven by a motor controller (C-863.11). The nanocapillary was installed on Z-direction piezo. The ion current was amplified by a trans-impedance amplifier (DLPCA-200, Femto, Germany). In order to decrease noise interference, the scanning head was shielded by a Faraday cage. The collection of ion current and the control of the piezo and motors were realized by the data acquisition card. The sampling frequency was set to 10 kHz. The scanning program was written in C++. The experimental data were processed by MATLAB R2018a, such as denoising, sampling and counting. The morphology image was achieved by filling the Z-axis piezo location of each pixel at ion current threshold into the corresponding XY coordinate; the modulus image was achieved by filling the modulus value calculated according to the ion current of each pixel at approaching destination into the corresponding XY coordinate. The images were processed by MATLAB R2018a, such as filtering and overlapping.

1.2. Cell Culture

MCF7 and SKOV3 (ATCC) cells were cultured in 35 mm cell culture dishes (Corning, USA). Roswell Park Memorial Institute (RPMI) 1640 medium supplemented with 10% fetal bovine serum and 1% penicillin-streptomycin (Gibco, Thermo Fisher Scientific) was used. After 24 h of culture at 37 °C with 5% CO₂, cells were located on the microscopy stage for SICM imaging. Before scanning, the solution was replaced by 2 mL 1X HEPES buffer (containing 8 g/L NaCl, 0.74g/L KCl, 0.27 g/L NaH₂PO₄·12H₂O, 1g/L glucose, 5g/L HEPES). 0.5 mM MgCl₂ and 1 mM CaCl₂ were added to promote cell adhesion.

1.3. Modulus imaging of the PDMS samples

Polydimethylsiloxane (PDMS, DOWSIL 184, US) base was mixed with an agent by a mass

ratio of 5:1, 10:1, 15:1, and 20:1. The mixtures were poured into the cylindrical mould with a diameter of 5 mm and a height of 5 mm. The samples were then put under 80 °C for 30 min. The modulus of these PDMS samples was tested using by Shore durometer. Then, the dish with the PDMS sample was installed on the sample stage of SICM. The nanocapillary (QF100-50-10, Sutter Instrument, CA, USA) was prepared using a P-2000 micropipette puller (Sutter Instrument). The pulling program was ‘Line 1: Heat 900 Fil 2 Vel 20 Del 120 Pul 90 Line 2 Heat 950 Fil 5 Vel 30 Del 130 Pul 160’. The nanocapillary was characterized by scanning electron microscopy (SEM, Hitachi S-4800, Japan). 200 mM KCl was injected into the nanocapillary and the dish. A bias of 0.2 V was applied between the two Ag/AgCl electrodes inside and outside the nanocapillary. The nanocapillary was localized above the PDMS samples with the help of an optical microscope. The samples were scanned using a hopping mode with a hopping height of 2 μm . The pixels in XY-direction were set to be 32×32 , and the step was set to be 1 μm . In a typical scan, the threshold is set to be 99% (98% for the hovering experiment). During the approaching process, the Z-axis location corresponding to the threshold (99%) was collected for morphology imaging. Then, the nanocapillary was controlled to move down with an impulsive displacement (typically 25%-50% of the tip inner diameter) at the same speed. The ion current at the terminal point was collected for modulus calculation. The viscosity, the approaching velocity and the threshold were chosen as parameters to verify the accuracy of the relationship between modulus and ion current. The viscosity was 0.001, 0.0015, 0.00239 and 0.00441 Pa·s by adding PEG-2000 into the solution. The approaching velocity was set to be 21, 27, 36, 49 and 61.5 $\mu\text{m/s}$, respectively. The ion threshold was set to be 98%, 95%, 90%, 85% and 80%, respectively. The modulus was calculated according to Equation (2) using MATLAB R2018a. The modulus image was obtained by filling the values of different scanning sites according to the corresponding XY locations.

1.4. Young’s Modulus imaging of single cells

The dish with cells was installed on the microscopy stage. The cell was scanned in HEPES buffer containing 0.5 mM MgCl_2 and 1 mM CaCl_2 . The nanocapillary was localized to the selected cell with the help of an optical microscope. For the scanning of the whole cell, the hopping height was set to 15 μm . The pixel in XY-direction was set to be 128×128 and the step was set to be 375 nm. The approaching velocity was set to be 20 $\mu\text{m/s}$, and the ion threshold was set to be 98%. For the scanning of the tiny area, the hopping height was set to 2 μm . The pixel in XY-direction was set

to be 128×128 and the step was set to be 20 nm. The approaching velocity was set to be 40 μm/s, and the ion threshold was set to be between 96% and 98%. After the scanning of a living cell, the nanocapillary was lifted out of the solution. Then, the physiological phosphate buffer saline (1X PBS) was replaced by 4% paraformaldehyde dissolved in HEPES buffer to fix the cell. After the 30-minute fixation, the 4% paraformaldehyde was replaced by HEPES buffer. Then, the same cell and the same tiny area were scanned again. For the overlapping of morphology and modulus images, the images were first binarized with a threshold of 50%. For example, pixels of the morphology image with a value greater than the average value were filled with red color, and others were filled with black color. Pixels of the modulus image with a value greater than the average value were filled with green color, and others were filled with black color. And the two images were overlapped, the yellow pixels resulted from the overlap of red and green pixels, which means the pixels have both a large height and Young's modulus.

1.5. Scratch wound healing assay

The scratch wound healing assay was performed to induce the migration of SKOV3 cells, a human ovarian cancer cell line. When SKOV3 cells reached approximately 90% confluence in a 3.5 cm petri dish, they formed a confluent monolayer of cells. At this point, a "scratch" was created in the cell monolayer to simulate a wound, inducing cell migration toward the wound area to investigate the healing process. To create a consistent and reproducible scratch, a sterile 2.5 μL pipette tip was used to scrape the cell monolayer in a straight line across the center of the well. Care was taken to apply uniform pressure to ensure that the scratch was of consistent depth and width. The pipette tip was moved in a single motion to minimize variability in the scratch width. After scraping, the cells were gently washed with 1X PBS to remove any detached cell debris, ensuring that the wound area was clean. The medium was then replenished with the fresh 2 mL complete culture medium. The scratch was observed and measured by the optical microscope using CCD (Dhyana 400BSI V3). The initial width of the scratch was 257 μm, which allows for a measurable gap for the cells to migrate into during the assay. Then the dish was placed into the culture incubator at 37 °C. After 2 hours, the width of the scratch was 247 μm, indicating a gradual migration of cells towards the scratch. After the cell migration assay, the dish was installed on the sample stage. The selected cell was scanned by SICM using the same parameters. Then the cells were fixed in 1X PBS buffer containing 4% paraformaldehyde for 30 min. After being washed by PBS three times, the

cells were permeabilized in 0.5% Triton X-100 in PBS for 10 minutes at room temperature. For the cell actin cytoskeleton stain, cells were labeled with SF488-phalloidin (Solarbio) at a 1:50 dilution in PBS for 20 minutes at room temperature. After being washed with PBS three times, nuclei were stained with DAPI solution (Beyotime) for 5 minutes at room temperature. Finally, the labeled cells were stored in 1X PBS. Fluorescence images were taken by a CCD. The exciting and emitting light wavelengths were 488 and 525 nm, respectively.

Mathematical relation between ion current and sample modulus

When the hopping mode of SICM is adopted, the nanocapillary moves downward and upward at every scanning site. The capillary will experience a force contrary to the motion direction which results from the outside solution. While there is no relative displacement between the nanocapillary and the inside solution. The friction (hydrodynamic resistance) should be the stiction, which is tiny enough to be ignored compared with the flow resistance and has been balanced by gravity and the capillary force. According to fluid mechanics during the approaching process, the hydrodynamic resistance between the nanocapillary and the solution can be described as: ^[S1]

$$f = \frac{1}{2} \rho C v^2 S \quad (\text{Equation S1})$$

where ρ is the solution density, v is the approaching velocity, and S is the sectional area. C is the drag coefficient that can be expressed as:

$$C = \frac{24}{Re} + \frac{3}{\sqrt{Re}} + 0.34 \quad (\text{Equation S2})$$

where Re is the Reynolds number. It is described as:

$$Re = \frac{\rho v d}{\eta} \quad (\text{Equation S3})$$

where η is the solution viscosity, which is typically 0.001 Pa·s for aqueous solution, and d is the characteristic length (tip outer diameter here). For a velocity of 50 $\mu\text{m/s}$, the Reynolds number Re is less than 0.05. If placing Re in the laminar flow region, the coefficient could be simplified to:

$$C = \frac{64}{Re} \quad (\text{Equation S4})$$

Accordingly, the force can be expressed as:

$$f = \frac{1}{2} \rho \frac{64\eta}{\rho v d} v^2 \frac{\pi d^2}{4} = 8\pi\eta v d \quad (\text{Equation S5})$$

Meanwhile, the surrounding solution will receive the isometric force in a downward direction. As the approaching speed is slow enough, it is located in the laminar flow region according to Equation S3. This phenomenon means the shape of the tip has few effects on the resulting force, including the cone angle, the sharp or round edge of the pipette tip. It could be totally applied to the sample surface when the nanocapillary-sample distance is tiny enough. As a result, the sample deformation will arise then. In this work, the force is applied by the nanocapillary, which can be regarded as a conical pressure head. According to the Sneddon model^[S2], the relationship between applied force and sample deformation can be described as:

$$f = \frac{2\tan\alpha}{\pi}\delta^2 E \quad (\text{Equation S6})$$

where α is the half-cone angle, δ is the sample deformation and E is the apparent Young's modulus. In this work, membrane modulus refers to the apparent Young's modulus, which is equivalent to Young's modulus under practical testing conditions.

For SICM, the ion current is the base for the morphology recognition. After being normalized, it can be described as:^[S3]

$$I = \frac{1}{\left(1 + \frac{3\ln\left(\frac{r_o}{r_i}\right)r_i\tan\alpha}{2x}\right)} \quad (\text{Equation S7})$$

where r_o is the capillary outer radius, and r_i is the capillary inner radius. x is the nanocapillary tip-sample distance, which could be affected by the deformation under the force:

$$x = d_0 + 2\pi\sqrt{\frac{\eta vd}{E\tan\alpha}} \quad (\text{Equation S8})$$

where d_0 is the nanocapillary-sample distance at the end of Z-axis displacement, which can be determined by the imaging results of standard samples. The minimum current is decided by the final nanocapillary tip-sample distance, which can be affected by the sample deformation. Also, it should be pointed out here that under low Re number, the continuity equation and Stokes equation for incompressible fluids can be simplified to a "one-dimensional flow model", with the pressure distribution along the axis given by:^{S4}

$$f(x) = f_0 e^{-\frac{2x}{d}} \quad (\text{Equation S9})$$

where f_0 is the hydrodynamic resistance force at the front face. The normalized f and δ trends are shown in Fig. S3. It can be observed that hydrodynamic resistance and sample deformation decrease rapidly (nearly reaching 0 when the distance is twice the tip diameter). Although the decay should be considered, the force applied to the cell surface is actually too tiny to be accurately quantified. Additionally, measuring the absolute tip-sample separation is always challenging. In this work, as mentioned in Equation S8, d_0 was determined from the imaging results of standard samples rather than through direct measurement. The introduction of this parameter also serves to correct the model. For one scanning, the capillary parameters are fixed, and one composite parameter can be adopted to simplify the equation:

$$T = \frac{3 \ln\left(\frac{r_o}{r_i}\right) r_i \tan \alpha}{2} \quad (\text{Equation S10})$$

Therefore, the relationship between the modulus and ion current is established:

$$I_{\min} = \frac{1}{1 + \frac{T}{d_0 + 2\pi \sqrt{\frac{\eta v d}{E \tan \alpha}}}} \quad (\text{Equation S11})$$

where I_{\min} is the minimum current, T is the parameter corresponding to nanocapillary features. The units of the parameters are listed as follows: I_{\min} (normalized ion current, dimensionless), T (length, nm), d_0 (length, nm), η (viscosity, Pa·s), v (approach velocity, m·s⁻¹), E (Young's modulus, Pa), and α (cone half-angle, dimensionless). For a typical scanning, the outer and inner diameters of the nanocapillary are 20 and 15 nm, respectively. The cone angle is 8°. The threshold is set to be 98%. Then, T is calculated to be 0.45 nm. As other parameters of Equation S11 are known, by measuring I_{\min} of PDMS samples with known modulus, d_0 can be calculated. While it should be pointed out that this calibration method is not accurate enough for quantification. Especially for samples with relatively high modulus, imprecise d_0 will result in higher relative error. Besides, as the hydrodynamic resistance applied to the sample is tiny, the deformation of samples with a high modulus will be too tiny to be detected by SICM. Therefore, the modulus imaging method in this work is suitable for biological samples with relatively low modulus.

Here is the vivid description of this modulus imaging method. When an object moves through a fluid, it will experience resistance. A common example is the wind resistance of a car in motion. In this work, during the approaching process, the nanocapillary moves through the aqueous solution and experiences the resistance that results from the friction with the solution. At the same time, the counterforce works on a solution, which has the same strength and opposite direction. As the approach speed is only about tens of microns per second, according to equation S5, the friction or the counterforce is only located at pN level. The counterforce will be transferred to the cell surface through the solution between the nanocapillary and the cell. While this effect has a working distance, cell deformation will only arise when the tip is close enough to the cellular membrane. A common example is that when we throw a punch at a piece of paper and brake before the paper, it will still waggle although we do not touch it. But when we brake prematurely, the paper will not waggle as

the distance between the paper and the punch is too large. According to the stress-strain relationship, with a constant modulus, tiny stress will result in tiny strain. Therefore, the tiny counterforce includes the tiny deformation of the cellular membrane.

(S1) D. Ni, Chapter 20 - Vehicle Modeling. *Traffic Flow Theory*, **2016**, 279-285.

(S2) I. N. Sneddon, The Relation Between Load and Penetration in The Axisymmetric Boussinesq Problem for a Punch of Arbitrary Profile. *Int. J. Engng Sci.* **1965**, 3, 47-57.

(S3) C. C. Chen, L. A. Baker, Effects of Pipette Modulation and Imaging Distances on Ion Currents Measured with Scanning Ion Conductance Microscopy (SICM). *Analyst* **2011**, 136, 90.

(S4) J. Happel, H. Brenner, Low Reynolds number hydrodynamics with special applications to particulate media. **1983**, DOI: 10.1007/978-94-009-8352-6.

COMSOL simulation using Finite Element Method (FEM)

To obtain the distribution of friction force around the nanocapillary tip, finite element numerical simulations were conducted. All simulations were performed using a commercial finite element analysis software (COMSOL). The physical field for the finite element analysis was defined as "Laminar Flow". The 3D geometric models of the capillary and the solution can be considered rotationally symmetric shapes. To simplify the finite element solution and reduce computational time, a 2D axisymmetric model was employed, as depicted in Figure S1A. The inner radius was denoted as r_i , the outer radius of the nanocapillary as r_o , the distance from the nanocapillary tip to the sample surface as h , the half-cone angle of the nanocapillary as θ , and the immersion depth of the capillary into the solution as l . Specific geometric parameters were listed in Table 1. The sidewalls were assumed to be ideal rigid bodies to further streamline the model. The analysis focused solely on the laminar viscous forces within the solution and at the boundaries, with boundary conditions specified at the liquid-solid interface. The mesh division was illustrated in Figure S1B, comprising 44,115 domain elements and 2,217 boundary elements.

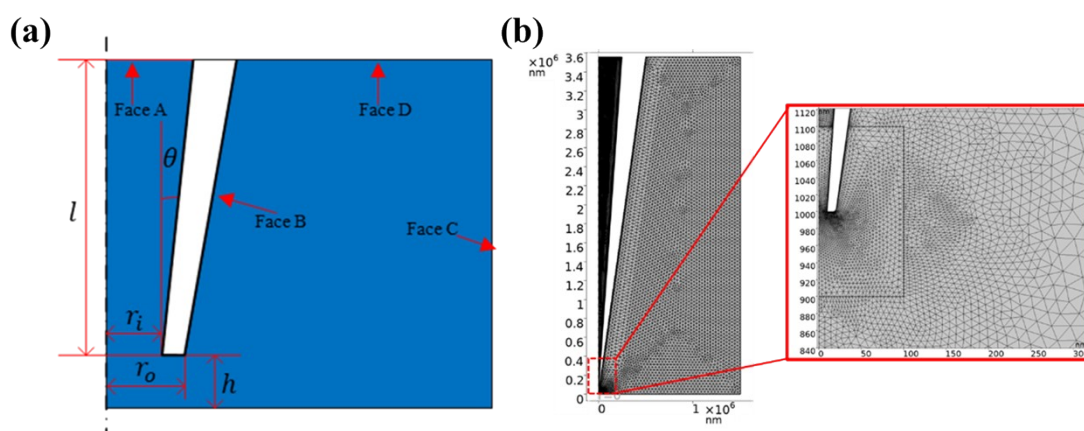


Fig. S1. Schematic diagram of rotational axis symmetry of the FEM model. (a) The schematic diagram and size (not to scale). (b) Simulation domain with grid (inset: a denser grid near the capillary tip).

Table S1. The primary geometric parameters of the pipette's FEM.

Parameter	Description	Value
r_i	Inner radius	7.5 nm
r_o	Outer radius	10 nm
h	Distance from nanocapillary tip to sample surface	1000 nm
θ	Half-cone angle of the pipette	8°
l	Nanocapillary immersion depth into the solution	3.5 mm

To obtain the distribution of frictional forces between the pipette and the solution, the Navier-Stokes equations were established within the solution region:

$$\rho(u \cdot \nabla)u = -\nabla p + \mu \nabla^2 u + F$$

where u represents the variable for fluid velocity; p represents the variable for pressure distribution; F represents external forces acting on the fluid; ρ represents the density of the solution (1000 kg/m^3); μ represents the dynamic viscosity of the fluid ($1 \times 10^{-3} \text{ Pa} \cdot \text{s}$). In addition, due to mass conservation within the fluid, the continuity equation must be satisfied:

$$\rho \nabla \cdot u = 0$$

The FEM boundary conditions were detailed in Table 2. Face A and Face D represent free liquid surface. Since the experiments were conducted at atmospheric pressure, the boundary condition was set as $p = 0$. Face B is where the solution contacts the sidewall of the pipette, and a downward probing velocity of $50 \text{ } \mu\text{m/s}$ is imposed. u is longitudinal to Face B. As θ is 8° here, u at Face B should be $-v \times \cos 8^\circ = -0.99v$, which is almost the same as $-v$. Besides, as the vertical component is blocked by Face B, u at Face B was approximated to be $-v$ in this work. Face C is the surface where the solution contacts the container, and it can be designated as a no-slip boundary condition with $u = 0$.

Table S2. Boundary conditions for the FEM model.

Boundary	Laminar Flow
Face A	$p = 0$
Face B	$u = -v$
Face C	$u = 0$
Face D	$p = 0$
Face E	$p = 0$
Face F	$u = -v$
Face G	$p = 0$

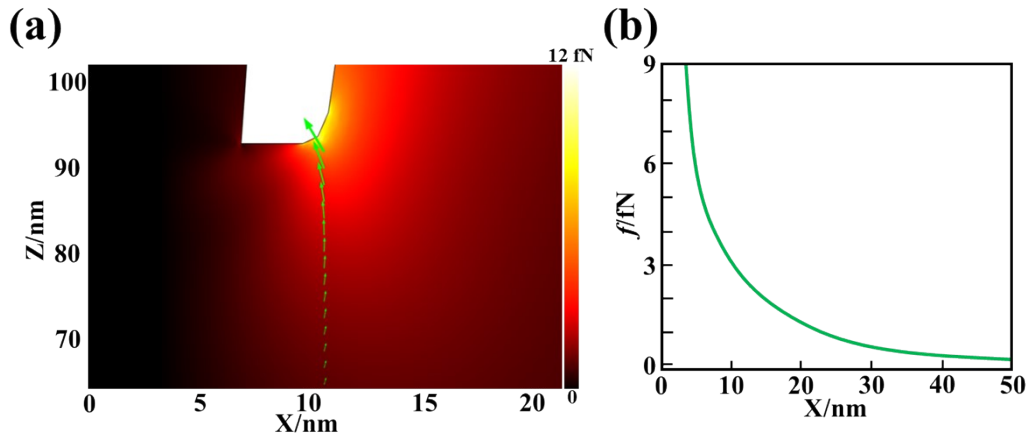


Fig. S2. (a) Simulation results of the friction force between the nanocapillary and solution with an outer diameter of 20 nm and an inner diameter of 10 nm. (b) Friction force distribution along the green arrows.

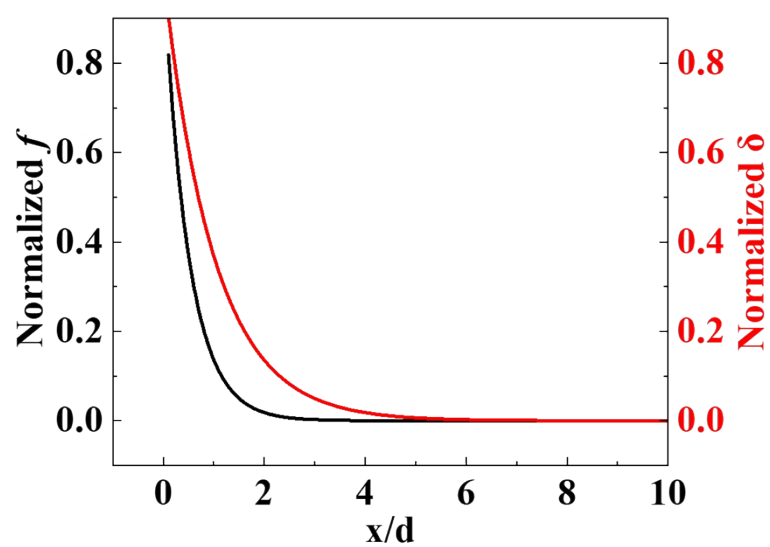


Fig. S3. The decay trend of hydrodynamic resistance and sample deformation with tip-sample separation.

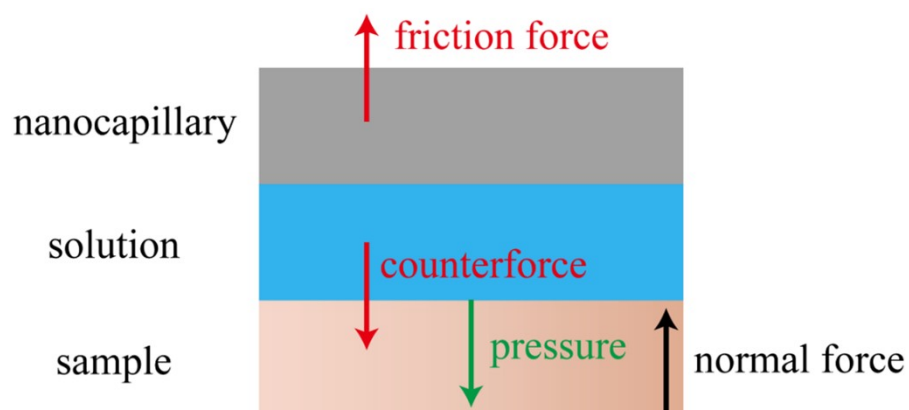


Fig. S4. Schematic diagram of the force transmission process during approaching.

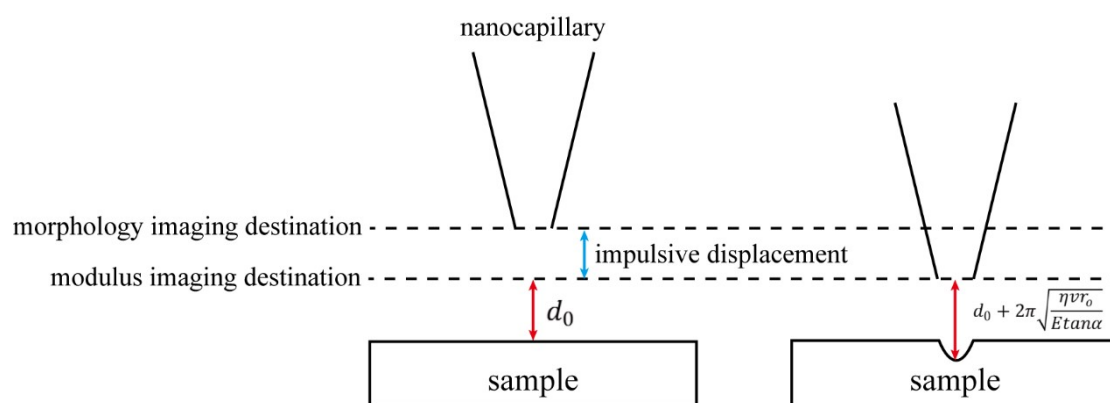


Fig. S5. Diagram of the morphology and modulus imaging destination.

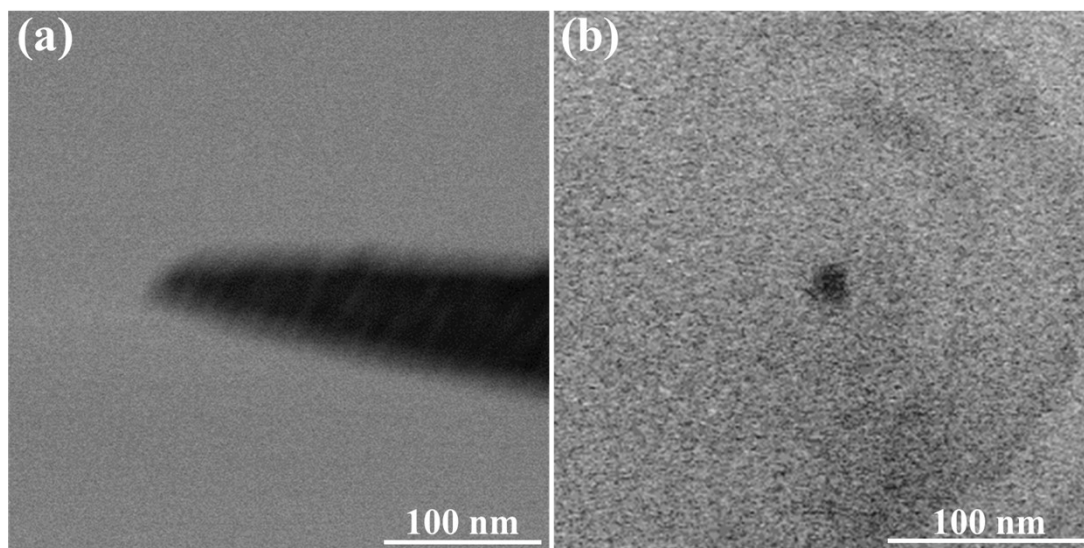


Fig. S6. SEM images of the nanocapillary (a) side view, (b) top view.

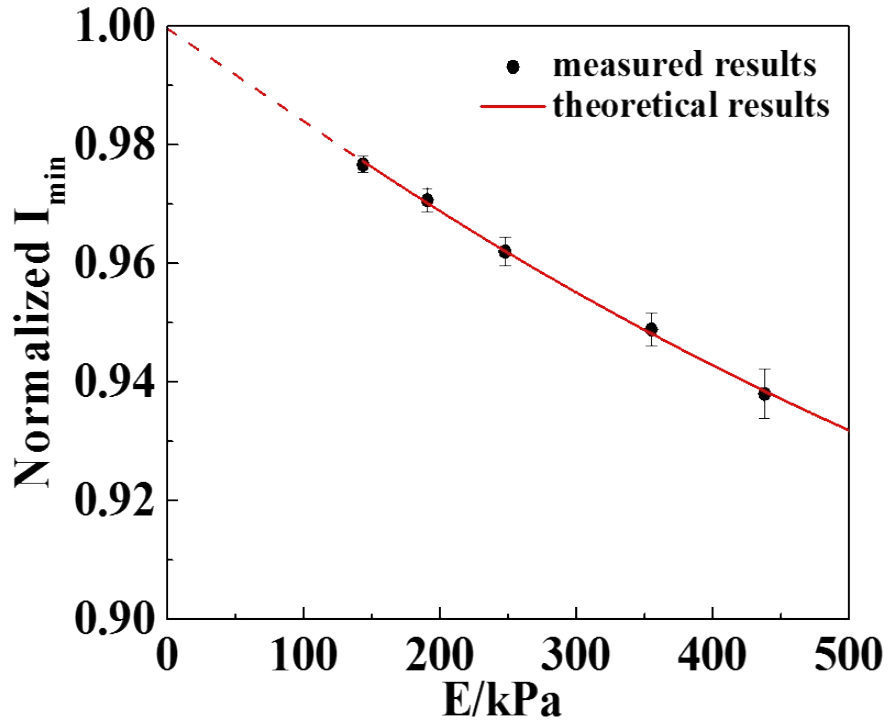


Fig. S7. Theoretical relationship (red line) and measured results of PDMS samples (black point) between I_{\min} and modulus. The error bar presents the standard deviation from the measurements at 1024 pixels (32×32).

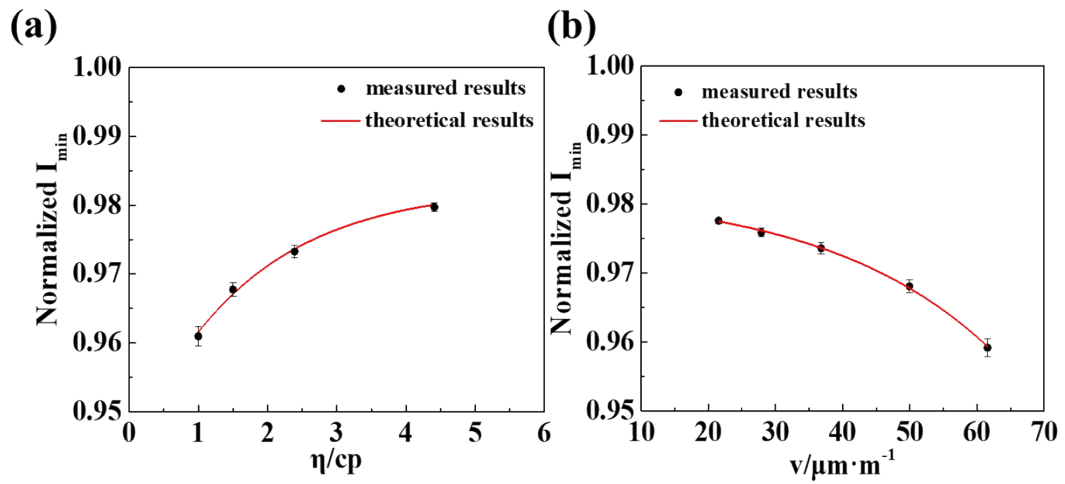


Fig. S8. (a) The relationship between I_{\min} and η with v of $60 \mu\text{m/s}$ and I_0 of 0.98. (b) The relationship between I_{\min} and v with η of 1 cp and I_0 of 0.98.

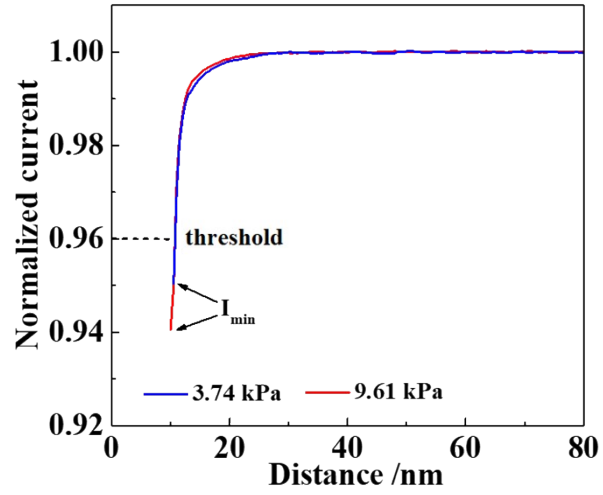


Fig. S9. The typical approaching curves of different sites of the cell surface with the calculated modulus of 3.74 and 9.61 kPa.

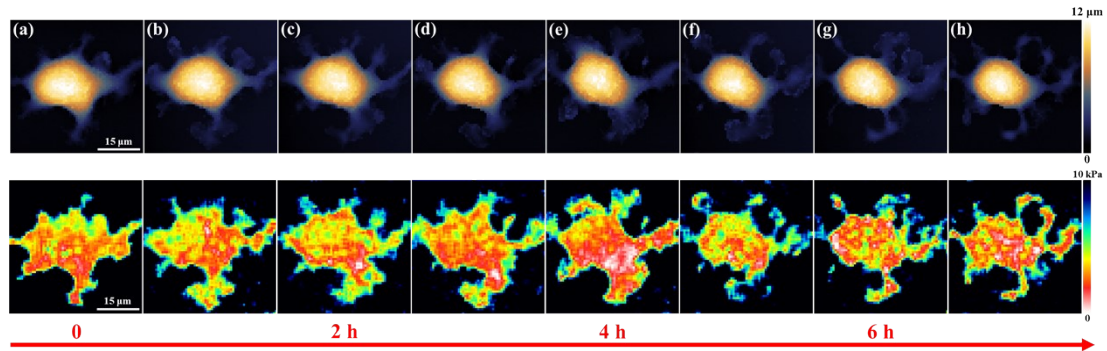


Fig. S10. Morphology and modulus images of the same cell during continuous scanning with a time interval of 1 h.

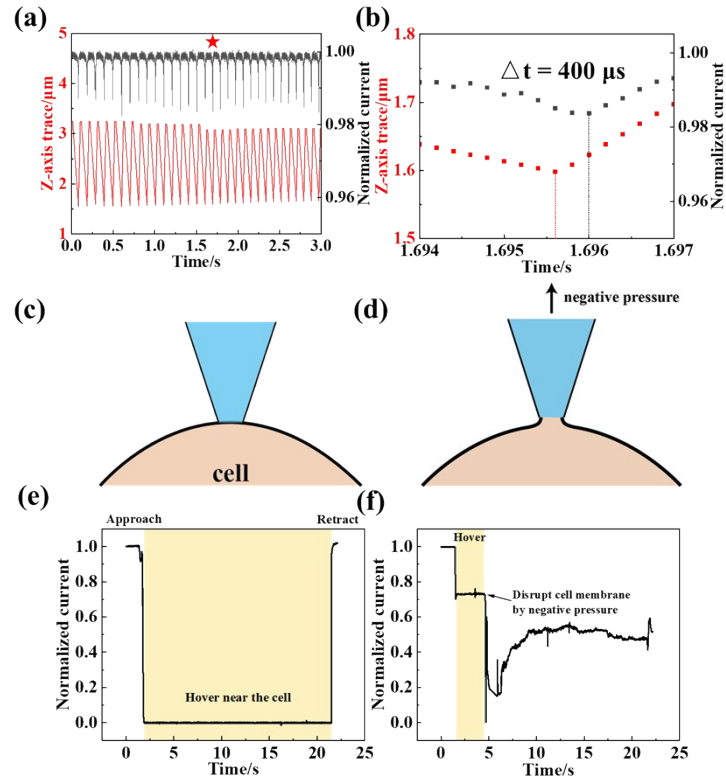


Fig. S11. (a) Z-axis trace and normalized current of multiple approach processes. (b) Z-axis trace and normalized current of a single approach (labeled by the red star). (c) Scheme and (e) ion current trace of the contact between tip and cell. (d) Scheme and (f) ion current trace of the membrane disruption process by negative pressure.

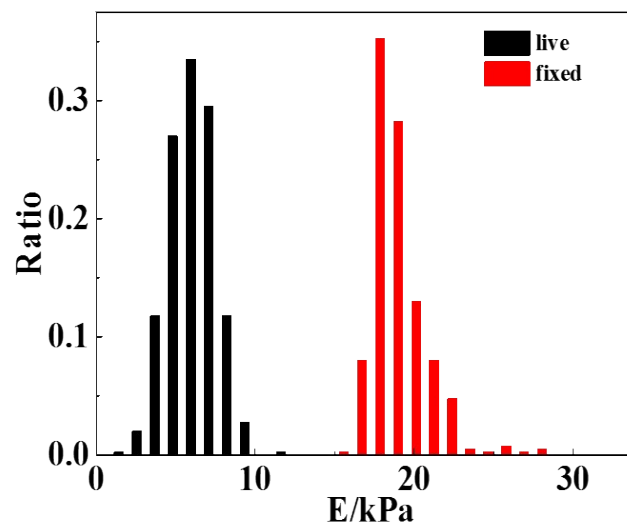


Fig. S12. Statistical results of cell modulus before and after fixation.

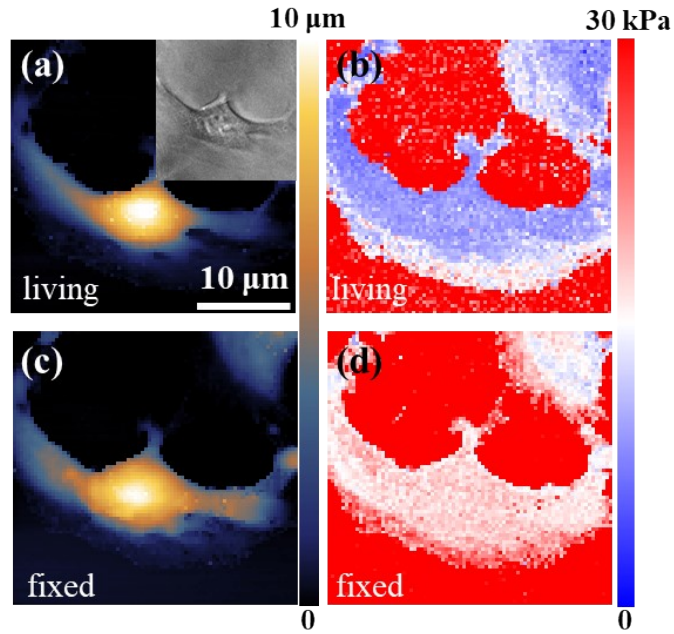


Fig. S13. SICM modulus imaging results of a single SKOV3 cell. SICM morphology images of the cell (a) before (inset is the bright field image of the chosen cell) and (c) after fixation; SICM modulus images of the cell (b) before and (d) after fixation.

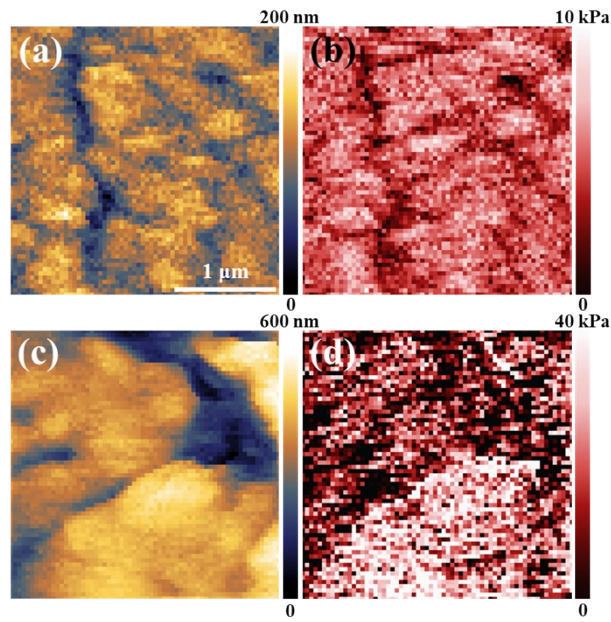


Fig. S14. SICM modulus imaging results of the tiny area on SKOV3 cells. SICM morphology images of the cell (a) before and (c) after fixation. SICM modulus images of the cell (b) before and

(d) after fixation.

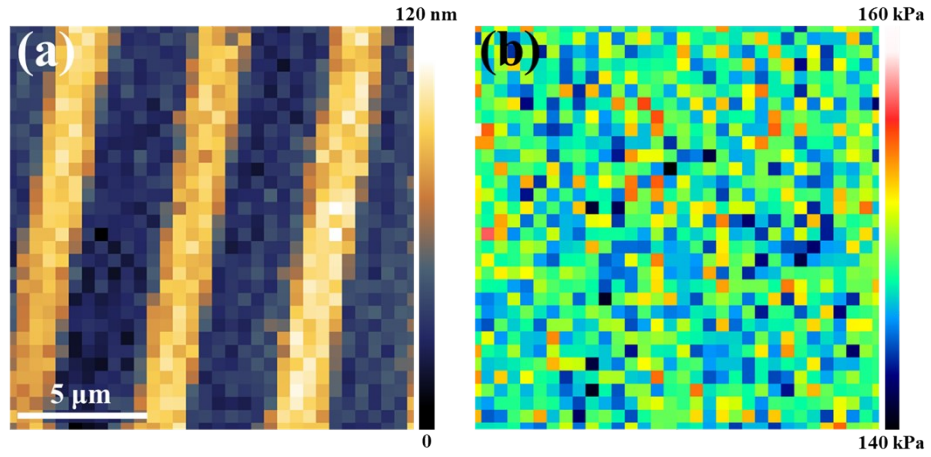


Fig. S15. SICM (a) morphology and (b) modulus image of the PDMS standard array.

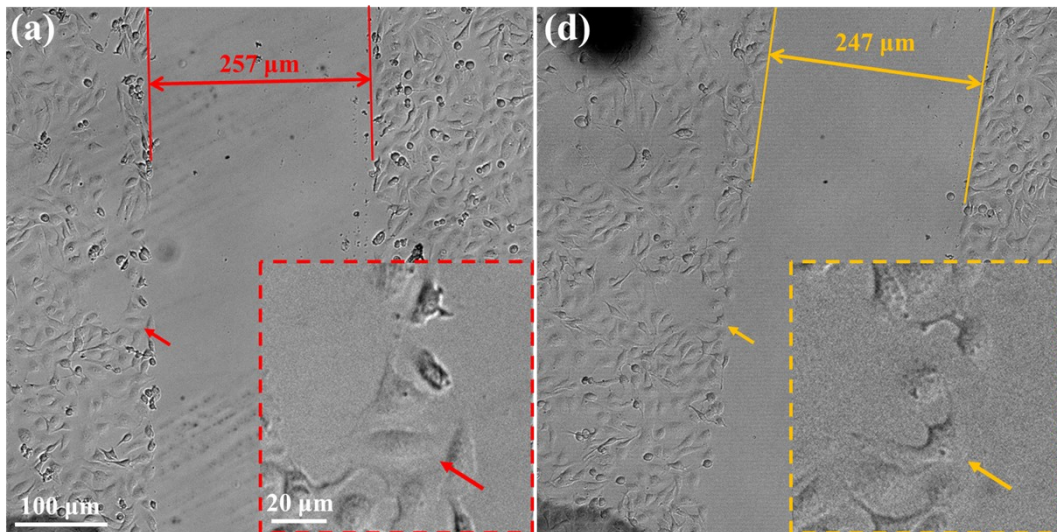


Fig. S16. Optical images of SKOV3 cells (a) before and (b) after wound healing assay for 2 h. The cell pointed by the red and orange arrows was chosen for SICM scanning.

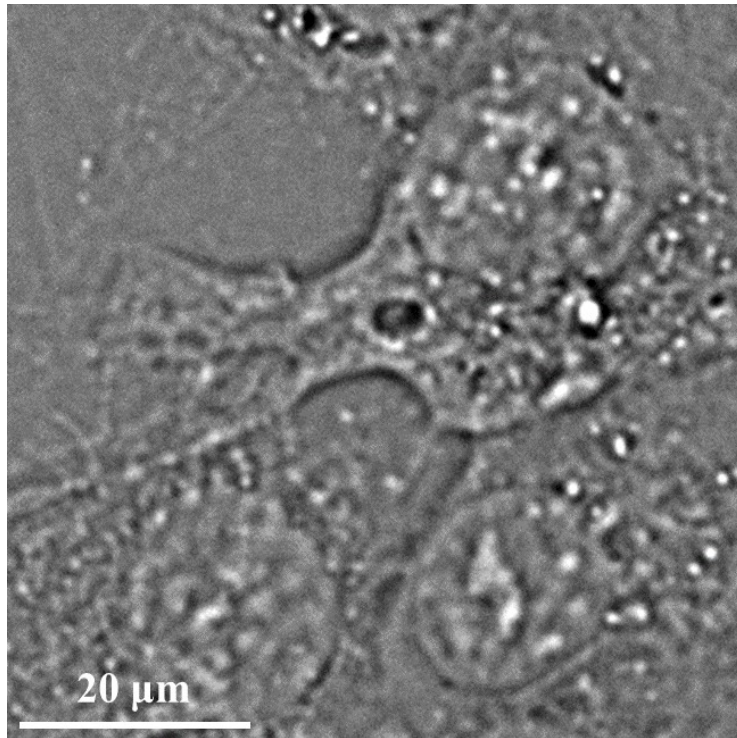


Fig. S17. Bright field image of the selected cell after fixation.